European Journal of Chemistry

Journal webpage: www.eurjchem.com

Study on the host-guest interactions during caffeine encapsulation into zeolite

Zvezdelina Lyubenova Yaneva [1], Manuela Stoyanova Staleva [2] and Nedyalka Valkanova Georgieva [1,*]

[1] *Chemistry Unit, Department of Pharmacology, Animal Physiology and Physiological Chemistry, Faculty of Veterinary Medicine, Trakia University, Students Campus, 6000 Stara Zagora, Bulgaria*
[2] *University "Prof. d-r Assen Zlatarov", 1 Prof. Yakim Yakimov Str., 8000 Bourgas, Bulgaria*

** Corresponding author at: Chemistry Unit, Department of Pharmacology, Animal Physiology and Physiological Chemistry, Faculty of Veterinary Medicine, Trakia University, Students Campus, 6000 Stara Zagora, Bulgaria.*
Tel.: +359.42.699642. Fax: +359.42.672009. E-mail address: nvgeorgieva@vmf.uni-sz.bg (N. Georgieva).

ARTICLE INFORMATION

DOI: 10.5155/eurjchem.6.2.169-173.1228

Received: 26 November 2014
Received in revised form: 06 January 2015
Accepted: 10 January 2015
Published online: 30 June 2015
Printed: 30 June 2015

KEYWORDS

Caffeine
Kinetics
Sorption
Equilibrium
Drug-delivery
Natural zeolite

ABSTRACT

The objective of this study was to investigate the equilibrium and kinetics behavior, sorption mechanism and host-guest interactions during caffeine (CAF) encapsulation in natural zeolite. The chemical, spectral and morphological properties of the newly obtained drug-carrier system were analyzed. Zeolite surface chemistry and morphology were characterized by determination of pH of zero charge, FT-IR and digital microscopy analyses. Equilibrium and kinetic sorption experiments and modeling were conducted to assess zeolite potential. Satisfactory extend of CAF encapsulation in the zeolite matrix (E 36.4%) was obtained. The probable host-quest interactions include Van der Waals interactions, H-bonds and chemical interactions between CAF functional groups and zeolite silanol groups, as well as parallel intraparticle diffusion of drug molecules in the mesopores of the mineral particles. The analyses of the experimental results indicated that natural zeolite could be successfully applied for encapsulating CAF.

Cite this: *Eur. J. Chem.* **2015**, *6(2)*, 169-173

1. Introduction

The wide structural and morphological diversity of different types of clay minerals offers unique opportunities for their potential applications in the veterinary and human medicine for encapsulation of various biologically-active substances. Furthermore, such system can also be employed in the modulation of safe and effective delivery of the drugs to specific body centers, for control of the release rate and regulation of the time profile of pharmaceutical formulations to achieve maximum therapeutic benefit [1-3].

The laboratory studies of Rimoli *et al.* [1] and Hadizadeh *et al.* [3] demonstrated the high potential of specific synthetic zeolitic matrices as drug delivery systems (DDS) with respect to ketoprofen [1] and ibuprofen [3]. The sorption behavior of timolol maleate™, a nonselective adrenergic blocker, was also investigated. The physicochemical characteristics of the formed TM-montmorillonite hybrid, analyzed by means of X-ray diffractional structure analyses, FT-IR spectroscopy and thermogravimetric analyses, as well as the biochemical behavior of the hybrid system, examined in simulated gastric (pH = 1.2) and intestinal fluid (pH = 7.4) at 37±0.5 °C, revealed controlled release of TM from the montmorillonite interlayer spaces [2]. A number of investigations demonstrated high adsorption capacity of various natural and modified organo-bentonites and palygorskite towards different antibiotics ampicillin [4], amoxicillin [5], oxytetracycline [6], tetracycline [7].

The present study was provoked by the lack of investigations regarding the applicability and potential of natural Bulgarian zeolite as a composite material for encapsulation of pharmaceutical substances.

The objective of this study was to investigate the equilibrium and kinetics behavior, sorption mechanism and host-guest interactions during caffeine (CAF) encapsulation into natural zeolite.

2. Experimental

2.1. Reagents

Caffeine anhydrous (1,3,7-trimethyl-1*H*-purine-2,6(3*H*, 7*H*)-dione), $C_8H_{10}N_4O_2$ (CAS No: 58-08-2) was supplied by Sigma-Aldrich (Fluka Analytical, >99% HPLC).

The natural zeolite used in the present study was supplied by Bentonite AD, Kurdzhali City, Bulgaria. The natural Bulgarian zeolite used in the present study characterized with

ISSN 2153-2249 (Print) / ISSN 2153-2257 (Online)
http://dx.doi.org/10.5155/eurjchem.6.2.169-173.1228

pore volume 0.11 cm^3/g, density 1.10 g/cm^3; specific surface area 37.1 m^2/g, and clinoptilolite content 87% [8].

2.2. Zeolite characterization

Prior to the sorption experiments, the mineral composite was thoroughly washed several times with distilled water to remove dust and any adhering substances. The washed material was oven dried at 373 K for 48 h. The prepared sample was stored in airtight containers for further studies. No other chemicals or physical treatments were applied prior to the sorption experiments. The used fraction was 0.5-1.5 mm.

The zero surface charge (pH_{PZC}) of zeolite was determined, using the solid addition method [9,10]. The microscope morphological analyses of zeolite were conducted by a digital microscope at 500× magnification.

2.3. UV/VIS spectrophotometry

CAF concentrations were measured with UV-VIS spectrophotometer DR 5000 Hach Lange, Germany, supplied with 10 mm quartz cells. All spectra were recorded in the UV region at λ 282 nm with 2 nm slit width, 900 nm/min scan speed and very high smoothing.

2.4. FT-IR spectroscopy

FT-IR spectra of fresh and CAF-loaded zeolite were obtained with KBr disc technique in the range 400-4000 cm^{-1} using TENSOR 37 Bruker FT-IR spectrometer (Bruker Optik GmbH, Germany). pH was measured on pH-meter Consort C931, Belgium.

2.5. Sorption studies

Equilibrium sorption experiments were carried out by agitating predetermined mass of zeolite with 100 cm^3 of CAF solutions with initial concentrations in the range 5-50 mg/dm^3 at temperature = 19±2 °C and pH = 7.5. The sorbate/sorbent systems were agitated until equilibrium. Then, the drug solutions were separated from the adsorbent by centrifugation with Heraeus Labofuge 200 (Thermo, Electron Corporation) at 5300 g for 20 min and filtered using 0.45 μm membrane filters (LCW 916, Hach Lange, Germany) to ensure the solutions were free from adsorbent particles before measuring the residual CAF concentration.

The corresponding values of CAF solid phase concentrations (q_e) were calculated by the mass balance equation Equation (1):

$$\left(C_o - C_e\right) \times V = \left(q_e - q_o\right) \times w \quad (1)$$

where C_o (mg/dm^3) is the initial caffeine concentration in the liquid phase, C_e (mg/dm^3) is the equilibrium caffeine concentration in the liquid phase, q_o= 0 and w (g) is the sorbent mass.

The kinetic experiments were conducted in a standardized batch adsorber with a two-bladed impeller [11] at initial CAF concentration C_o 5 mg/dm^3, and masses of zeolite w 3 g and 6 g at agitation rate n 200 rpm, temperature = 19±2 °C and pH = 7.5.

All experiments were carried out in triplicate, and the average values were taken to minimize random error. Blanks containing no adsorbate and replicates of each adsorption point were used for each series of experiments.

3. Results and discussion

3.1. Caffeine characterization

Caffeine standard solutions, in the concentration range C_o 3-50 mg/dm^3, were prepared in distilled water. CAF calibration curve in the studied concentration range characterized with very high linearity r^2 = 0.9994. Chemically, caffeine could be classified as belonging to the heterocyclic group of compounds called the purines. Its molecule is achiral without stereoisomers. The two amide groups exist predominately as zwitterionic resonance structures where N and C atoms are double bonded to each other so that both of these N atoms are planar (sp^2 orbital hybridization) (Figure 1). The fused ring system therefore contains ten π-electrons and hence according to Hückel's rule [12] is aromatic. Besides, it is weakly basic (pK_a = ~0.6) requiring strong acid to protonate it.

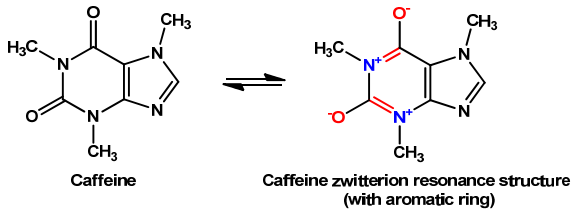

Figure 1. Zwitterion resonance structure of CAF.

3.2. Zeolite characterization

The analyses established zero surface charge of zeolite at pH = 7.34. Hence, the pH_{PZC} is 7.34 (Figure 2). The digital microscope images of the fresh zeolite (Figure 2) displayed the heterogeneity of the mineral surface.

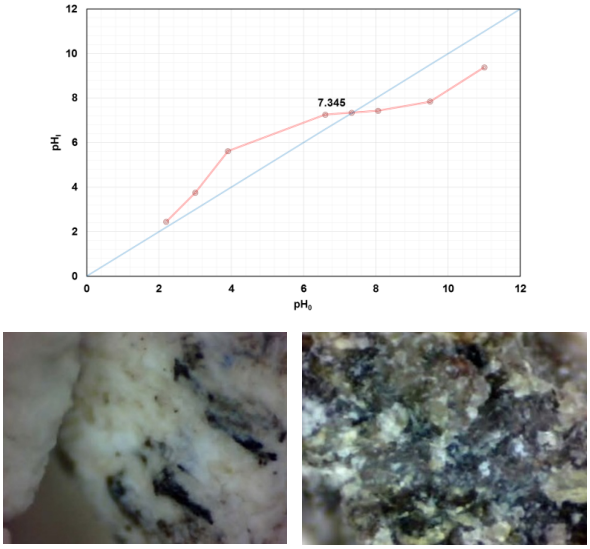

Figure 2. pH_{PZC} and digital microscope images (500×) of fresh Bulgarian zeolite.

3.3. Sorption equilibrium

The experimental data of CAF sorption by zeolite were described by the Langmuir, Freundlich and Redlich-Peterson models [13] (Figure 3).

The values of the calculated isotherm parameters, correlation coefficients are presented in Table 1. The maximum equilibrium capacity of the mineral material towards CAF was q_{max} = 0.42 mg/g, while the monolayer capacity according to the Langmuir model defined as K_L/a_L was 0.69 mg/g.

Table 1. Values of Langmuir, Freundlich and Redlich-Peterson isotherm constants and correlation coefficients for the system CAF-zeolite

Equilibrium model	Equilibrium modelling / Model equations	Model parameters	r^2
Langmuir	$q_e = \frac{K_L c_e}{1+a_L c_e}$ (2)	K_L = 0.023 dm³/mg a_L = 0.0335 g.dm³/mg²	0.7055
Freundlich	$q_e = K_F . c_e^{n_F}$ (3)	K_F = 0.0361 dm³/g n_F = 0.6599	0.8994
Redlich-Peterson	$q_e = \frac{K_R . c_e}{1 + a_R c_e^{b}}$ (4)	K_R = 0.0361 dm³/g a_R = 0.2447 1/mg b_R = 0.6390	0.7290

Table 2. Values of the parameters derived from pseudo-first order (PFO)/pseudo-second order (PSO)/intraparticle diffusion (ID)/mixed pseudo-first/pseudo-second order (MFSO) models for the system CAF-zeolite.

Kinetic/mass transfer models		*w = 3 g*	*w = 6 g*
PFO model [15]			
Non-linear form $\frac{dq_t}{dt} = k_1(q_e - q_t)$ (5)	*Linear expression* $\log(q_e - q_t) = \log q_e - \frac{k_1}{2.303} t$ (6)	k_1 = 0.0545 1/min q_{e1} = 0.242 mg/g R_1^2 = 0.9214	k_1 = 0.0435 1/min q_{e1} = 0.114 mg/g R_1^2 = 0.8929
PSO model [16]			
Non-linear form $\frac{dq_t}{dt} = k_2(q_e - q_t)^2$ (7) $\frac{1}{q_e - q_t} = \frac{1}{q_e} + k_2 t$ (8)	*Linear expression* $\frac{t}{q_t} = \frac{1}{k_2 q_e^2} + \frac{1}{q_e} t$ (9)	k_2 = 0.3634 g/(mg.min) q_{e2} = 0.346 mg/g R_2^2 = 0.9945	k_2 = 1.1237 g/(mg.min) q_{e2} = 0.245 mg/g R_2^2 = 0.9987
ID model [17]			
Non-linear form $q_t = k_i t^{0.5} + I$ (10)		k_{ID}' = 0.0194 mg/(g.min$^{0.5}$) I' = 0.1402 $R_{ID}'^2$ = 0.9485 k_{ID}'' = 0.0048 mg/(g.min$^{0.5}$) I'' = 0.2738 R''² = 0.9134	k_{ID}' = 0.0122 mg/(g.min$^{0.5}$) I' = 0.1465 $R_{ID}'^2$ = 0.9947 k_{ID}'' = 0.0072 mg/(g.min$^{0.5}$) I'' = 0.1721 R''² = 0.8944
MFSO model [18]			
Non-linear form $q = q_e\left(\frac{1-\exp(-k_1 t)}{1-f_2\exp(-k_1 t)}\right)$ (11)	*Linear expression* $\ln\left(\frac{1-F}{1-f_2 F}\right) = -k_1 t$ (12) where $F = \frac{q_t}{q_e}$ $f_2 = \frac{k_2 q_e}{k_1 + k_2 q_e}$ (13)	R_M^2 = 0.9662	R_M^2 = 0.9891

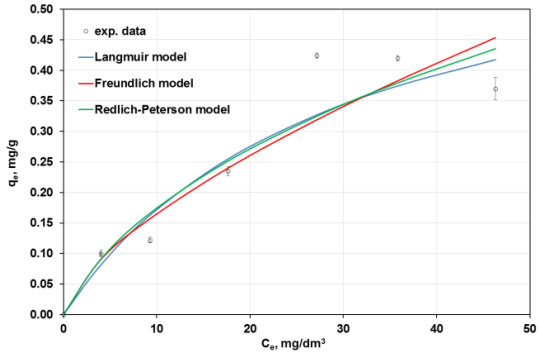

Figure 3. Experimental and model equilibrium isotherms for the hybrid CAF-zeolite system.

Obviously, Freundlich isotherm characterized with the highest r^2 value (r^2 = 0.8994, Table 1) indicating the applicability of this empiric equation with regard to the experimental equilibrium data. The favorable nature of CAF sorption by zeolite was confirmed by the fact that $1/n_F > 1$. The high extend of correlation, however, outlines the heterogeneity of the sorbent with interaction between adsorbed molecules with a non-uniform distribution of the heat of sorption depicting multilayer adsorption of the drug molecules on the solid surface and into the pores of the sorbent.

3.4. Sorption kinetics

The experimental kinetic curves, plotted as $q_t = f(t)$ (Figure 4), displayed that the sorption rate in the initial stages of the process was the highest. The system reached equilibrium approximately 80 min after the beginning of the process. The highest adsorption capacity attained was q_e = 0.32 mg/g. The experimental data were modeled by the pseudo-first order (PFO), pseudo-second order (PSO) [14], the mixed pseudo-first/pseudo-second (MFSO) order kinetic models, as well as by the intraparticle diffusion (ID) model (Table 2).

The highest values of the correlation coefficients (R_2^2 > 0.9945), the approximately equal values of the calculated (q_{e2}) by the PSO model and the experimentally obtained equilibrium adsorption capacities (q_{exp}) (Table 2), proved the better applicability of the second order model, especially in the initial stages of the sorption process.

The MFSO model also correlated the experimental data satisfactorily, especially in the higher concentration ranges. Both kinetic models applied, however, do not identify the diffusion mechanism. Thus, the kinetic data were also analyzed by the ID model. The plot of q_t *vs* $t^{0.5}$ consisted of only two linear sections, presuming the presence of macro- and mesopores in the sorbent structure. As the values of R_{ID}^2 were higher than R_1^2 and commensurable with R_2^2 (Table 2), an explicit conclusion whether chemisorption or intraparticle diffusion was the general rate controlling mechanism during

CAF sorption on zeolite could not be withdrawn. Thus, more detailed discussion based on the nature of the probable zeolite-CAF interactions and FTIR analyses was made.

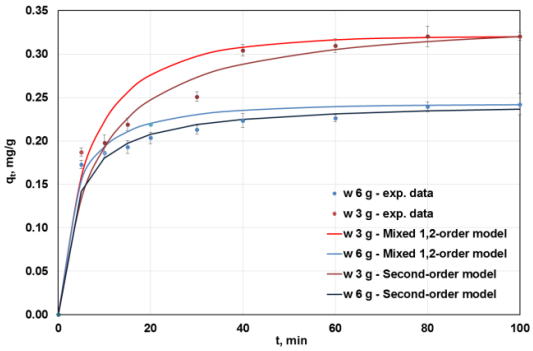

Figure 4. Comparison of the applicability of the pseudo-second-order model and mixed 1,2-order model models to the experimental data of CAF sorption on zeolite (C_o = 5 mg/dm^3; w = 3 g, 6 g; n = 200 rpm).

3.5. FT-IR analyses of fresh and caffeine-loaded zeolite

In the FT-IR spectra of fresh and CAF-loaded zeolite (Figure 5), the bands with a peak at 3445 cm^{-1} were assigned to OH-stretching, and the vibrations at 1637 cm^{-1} were referred to bending vibration of adsorbed water molecules associated with K and Ca in the channels and cages in the zeolite structure. The 1207 and 1049 cm^{-1} bands corresponded to asymmetric stretching vibration modes of internal T-O bonds in TO_4 tetrahedra (T = Si and Al). The 792 and 727 cm^{-1} bands were assigned to the stretching vibration modes of O-T-O groups and the bending vibrations of T-O bonds, respectively [19].

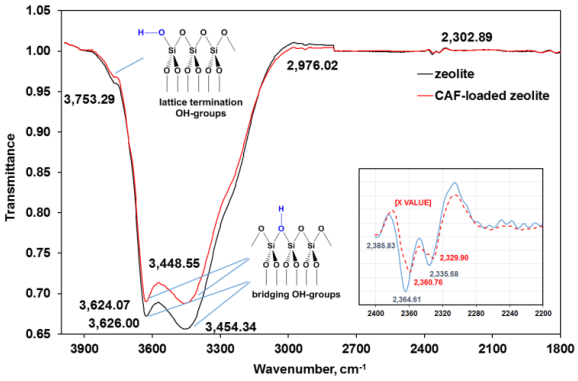

Figure 5. FT-IR spectra of fresh zeolite (Z) CAF-Z hybrid system. Inserts: enlarged region of intersection at 2400-2200 cm^{-1}.

Two types of OH-groups are present in the Bulgarian zeolite, including lattice termination silanol groups (~3745 cm^{-1}), located on the external surface, and bridging OH-groups with Bronsted acidity (~3630 and 3560 cm^{-1}) (Figure 5).

The well-resolved strong bands in the 1120-1000 cm^{-1} region were attributed to the presence of Al(III) in the octahedral position (Figure 5). Most of the octahedral sites were occupied by divalent central atoms, thus the O-H bending bands were shifted to wavenumbers in the 700-600 cm^{-1} range [20].

The incorporation of the pharmaceutically active compound CAF in zeolite displayed variations in the intensity of relevant bands on the FT-IR spectra of the CAF-loaded zeolite. In addition to the strong bands caused by the host zeolite, the FT-IR spectra for the system CAF-encapsulated-zeolite exhibited shifting of the bands in the region 2500-2000 cm^{-1} to lower frequencies (Figure 5). Besides, the vibrational bands at 3624 and 3442 cm^{-1}, which were attributed to adsorbed water, and the band at 1637 cm^{-1}, characteristic of C=O vibration/C=C bonding/C=N bonding, characterized with lower transmittances. The broadening of the vibrational bands in CAF-zeolite spectrum that occurred in the region 2958-2898 cm^{-1} could be attributed to the C-H stretching vibrations of the drug molecules [21].

Although for the prepared drug-carrier system, the FT-IR spectra were dominated by the strong bands assigned to the vibration of the zeolite structure and the characteristic CAF FT-IR vibrational bands in the CAF-zeolite spectra were weak, they provided evidence for the presence of the drug in the zeolite. Tomeckova *et al.* [22] and Amorim *et al.* [23] obtained similar results.

3.6. Host-guest interactions

The probable host-quest interactions during CAF encapsulation in zeolite include van der Waals interactions and H-bonds established between the O and N atoms from the C=O and C=N groups in CAF and the zeolite hydroxyls. The software package CS Chem 3D ultra was used to calculate the Connolly molecular surface area of CAF molecule 185.475 Å^2. The molecular radius of caffeine is estimated as 0.376 nm (Figure 6) [24].

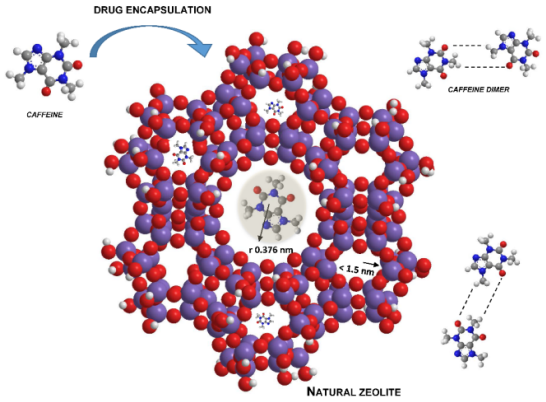

Figure 6. Spatio-geometrical aspects of CAF encapsulation into the zeolite matrix.

The comparison of the dimensions of CAF molecules with those of zeolite channels and pores: micropores (<1.5 nm) and (ii) mesopores (1.5-16.0 nm), revealed that there were no spatial limitations for the drug molecules to enter the micro- and mesopores of the zeolitic matrix (Figure 6). However, a number of scientific investigations revealed the tendency of self-association of CAF molecules, as well as the formation of stable dimers in aqueous solutions, especially at high concentrations [25], involving stacking interactions [26,27]. Consequently, the latter phenomenon could explain the observed lower values of the intraparticle diffusion correlation coefficients and rate constants as compared to those obtained for the PSO model.

Probably, the physical-chemical interactions and diffusion mechanisms evaluated concerned predominantly the outer surface of the natural Bulgarian zeolite, which also included the mesoporosity.

4. Conclusion

The sorption behavior of the studied drug/zeolite system could be explained by physical sorption at the beginning of the process, followed by the formation of H-bonds and chemical

interactions between CAF functional groups and zeolite silanol groups during the later stages of the encapsulation process, and parallel intraparticle diffusion of CAF molecules in the mesopores at the outer surface of the mineral particles.

Considering the unique properties of zeolite and the opportunities for its potential applications in the veterinary and human medicine, together with the satisfactory extend of CAF encapsulation in the zeolite matrix E 36.4% (C_o = 5 mg/dm^3, C_z = 7.5 g/dm^3) obtained in the present preliminary study, it could be concluded that the natural Bulgarian zeolite could be successfully applied for encapsulating CAF.

Acknowledgements

The study was supported financially by Project No. 4 OUP, "Determination of the contents of newly-synthesized drug substances and priority contaminants in model aqueous solutions and investigation of the possibilities of their removal by abundant and low-cost natural adsorbents", Trakia University, Stara Zagora, Bulgaria.

References

[1]. Rimoli, M. G.; Rabaioli, M. R.; Melisi, D.; Curcio, A.; Mondello, S.; Mirabelli, R.; Abignente, E. *J. Biomed. Mater. Res. A* **2008**, *87(1)*, 156-164.
[2]. Joshi, G. V.; Kevadiya, B. D.; Patel, H. A.; Bajaj, H. C.; Jasra, R. V. *Int. J. Pharm.* **2009**, *374*, 53-57.
[3]. Hadizadeh, F.; Khodaverdi, E.; Shandiz, R. H. Iran Int. Zeolite Conf. 2nd IIZC, April 29-30, 2010**,** Tehran.
[4]. Rahardjo, A. K.; Susanto, M. J. J.; Kurniawan, A.; Indraswati, N.; Ismadji, S. *J. Hazard. Mater*. **2011**, *190*, 1001-1008.
[5]. Budyanto, S.; Soedjono, S.; Irawaty, W.; Indraswati, N. *J. Environ. Prot. Sci*. **2008**, *2*, 72-80.
[6]. Barbooti, M. M.; Al-Bassam, K. S.; Qasim, B. H. *Iraqi J. Sci.* **2012**, *53(3)*, 479-486.
[7]. Chang, P. H.; Yua, T. L.; Munkhbayer, S.; Kuo, T. H.; Hung, Y. C.; Jean, J. S.; Lin, K. H. *J. Hazard. Mater***.** **2009**, *165*, 148-155.
[8]. Allen, S. J.; Ivanova, E.; Koumanova, B. *Chem. Eng. J*. **2009**, *152*, 389-395.
[9]. Hameed, B. H. *J. Hazard. Mater*. **2010**, *162*, 939-994.
[10]. Yaneva, Z.; Georgieva, N. *Macedonian J. Chem. Chemical Eng.* **2013**, *32(1)*, 133-149.
[11]. Koumanova, B.; Peeva-Antova, P. *J. Hazard. Mater*. **2002**, *90(3)*, 229-234.
[12]. Agyemang-Yeboah, F.; Oppon, S. Y. Topical Series in Health Science 1 (TSHS-1), Kerala, India, 27-37, 2013.
[13]. Hammud, H.; Chahine, M.; Hamaoui, B.; Younes, H. *Eur. J. Chem.* **2013**, *4(4)*, 425-433.
[14]. Lu, J.; Wu, M.; Yang, X.; Dong, Z.; Ye, J.; Borthakur, D.; Sun, Q.; Liang, Y. *J. Food Eng.* **2010**, *97*, 555-562.
[15]. Lagergren, S. *Kungliga Svenska Vetenskapsakademiens. Handlingar* **1898**, *24*, 1-39.
[16]. Ho, Y. S.; McKay, G. *Adsorp. Sci. Tech.* **1998**, *16*, 243-255.
[17]. Chien, S. H.; Clayton, W. R. *Soil Sci. Soc. Am. J.* **1980**, *44*, 265-268.
[18]. Haerifar, M.; Azizian, S. *J. Phys. Chem. C* **2012**, *116*, 13111-13119.
[19]. Mansouri, N.; Rikhtegar, N.; Panahi, H. A.; Atabi, F.; Shahraki, B. K. *Env. Prot. Eng.* **2013**, *39(1)*, 139-152.
[20]. Stuart, B. Infrared Spectroscopy: Fundamentals and Applications, John Wiley & Sons, West Sussex PO19 8SQ, England, 2004.
[21]. Verma, R.; Kumar, L. *J. Chem. Pharm. Res.* **2010**, *2(4)*, 194-198.
[22]. Tomeckova, V.; Rehakova, M.; Mojzisova, G.; Magura, J.; Wadsten, T.; Zelenakova, K. *Micropor. Mesopor. Mat.* **2012**, *147*, 59-67.
[23]. Amorim, R.; Vilacca, N.; Martinho, O.; Reis, R. M.; Sardo, M.; Rocha, *J. J. Phys. Chem. C* **2012**, *116*, 25642-25650.
[24]. Banerjee, S.; Verma, P. K.; Mitra, R. K.; Basu, G.; Pal, S. K. *J. Fluoresc*. **2012**, *22*, 753-769.
[25]. Yakovishin, L. A.; Borisenko, N. I.; Vetrova, E. V.; Rudnev, M. I.; Grishikovets, V. I. *Chem. Plant Raw Mat.* **2010**, *3*, 7-70.
[26]. Yakovishin, L. A.; Borisenko, N. I.; Vetrova, E. V.; Rudnev, M. I.; Grishikovets, V. I. *Russian J. Bioorg. Chem.* **2011**, *37(7)*, 858-861.
[27]. Son, S. Y.; Bui, M.; Racette, R. C.; Williams, J. E. *Chemical Sci. J.* **2013**, *2013*, 96, 1-3.